

# Magic Numbers in DNA-Stabilized Fluorescent Silver Clusters Lead to Magic Colors

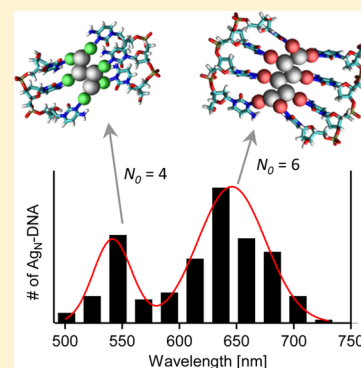
Stacy M. Copp,<sup>†</sup> Danielle Schultz,<sup>‡</sup> Steven Swasey,<sup>‡</sup> James Pavlovich,<sup>‡</sup> Mark Debord,<sup>†</sup> Alexander Chiu,<sup>†</sup> Kevin Olsson,<sup>†</sup> and Elisabeth Gwinn<sup>\*,†</sup>

<sup>†</sup>Physics Department, University of California Santa Barbara, Santa Barbara California 93117, United States

<sup>‡</sup>Chemistry Department, University of California Santa Barbara, Santa Barbara California 93117, United States

## S Supporting Information

**ABSTRACT:** DNA-stabilized silver clusters are remarkable for the selection of fluorescence color by the sequence of the stabilizing DNA oligomer. Yet despite a growing number of applications that exploit this property, no large-scale studies have probed origins of cluster color or whether certain colors occur more frequently than others. Here we employ a set of 684 randomly chosen 10-base oligomers to address these questions. Rather than a flat distribution, we find that specific color bands dominate. Cluster size data indicate that these “magic colors” originate from the existence of magic numbers for DNA-stabilized silver clusters, which differ from those of spheroidal gold clusters stabilized by small-molecule ligands. Elongated cluster structures, enforced by multiple base ligands along the DNA, can account for both magic number sizes and color variation around peak wavelength populations.



**SECTION:** Physical Processes in Nanomaterials and Nanostructures

Ligand-stabilized metal nanoclusters are an exciting class of materials due to their remarkable chemical, electrical, and optical properties<sup>1,2</sup> and promise for applications in catalysis,<sup>2,3</sup> nanoelectronics,<sup>1</sup> and biosensing.<sup>2</sup> Ligands enable cluster sizes that are not otherwise stable in solution.<sup>3</sup> The physical, chemical, and optical properties of a ligand-stabilized metal cluster are intimately connected to the properties of the ligand itself. Ligand–metal bonds at the cluster surface can even dictate the so-called “magic numbers” of gold clusters that occur due to enhanced stability of certain clusters with select numbers of metal atoms, reflecting electronic shell closings.<sup>4,5</sup>

Most ligand-stabilized noble metal nanoclusters have quasi-spherical geometries. However, a new class of DNA-stabilized silver clusters<sup>6</sup> ( $\text{Ag}_N\text{-DNA}$ ) displays evidence for rod-like shapes,<sup>7</sup> an exciting feature due to the possibility of new functionalities based on shape-tuned color and anisotropic polarization response. The challenge of isolating these small fluorescent clusters, which are surrounded by bulky DNA ligands, was recently overcome,<sup>8,9</sup> enabling identification of total silver content as  $N = 10\text{--}24$  Ag atoms, with 1–2 DNA oligomers associated with each cluster.<sup>9</sup> Reported optical properties of  $\text{Ag}_N\text{-DNA}$  vary widely, depending on DNA strand specifics.<sup>9</sup> Some are brightly fluorescent, with narrow-band emission wavelengths spanning the visible and near-IR<sup>10</sup> and quantum yields exceeding 90%.<sup>7</sup> High photostabilities have also been reported.<sup>11</sup> Due to these unique fluorescence properties,  $\text{Ag}_N\text{-DNA}$  are now employed in a number of fascinating sensing applications, including detection of metal ions,<sup>12,13</sup> microRNAs,<sup>14,15</sup> target DNA strands in the presence

of serum,<sup>16</sup> and single base mutations relevant to human diseases.<sup>17,18</sup>

Despite this growing list of applications, little is known about the origins of cluster color in  $\text{Ag}_N\text{-DNA}$ . Strategies for selecting cluster-stabilizing DNA oligomers generally focus on experimentally testing small sets of cytosine (C)-rich or guanine (G)-rich oligomers, which are important for forming fluorescent products,<sup>19–21</sup> to find sequences that produce attributes appropriate to a specific application. Here we instead use a large set of 684 distinct 10-base oligomers with widely varying composition to probe the origins of clusters with varying colors. We randomly selected sequences containing at least three total C plus G bases from a larger set produced using a random number generator with equal probability of placing A, C, G, or T bases at each site. Sequences containing less than a total of three C plus G bases were excluded to increase the probability of obtaining fluorescent  $\text{Ag}_N\text{-DNA}$  solutions, which only slightly changes the base content of the random sequence set (see Supporting Information Figure S1).

Robotic parallel synthesis of  $\text{Ag}_N\text{-DNA}$  under identical conditions was performed in well plate format (Figure 1b). In each well, the hydrated DNA oligomer was mixed with  $\text{AgNO}_3$ , followed by  $\text{NaBH}_4$  reduction. All clusters were excited via the DNA bases using 280 nm excitation.<sup>10</sup> The fluorescence spectra of resulting products were fitted to single Gaussian

**Received:** January 22, 2014

**Accepted:** February 27, 2014

**Published:** February 27, 2014

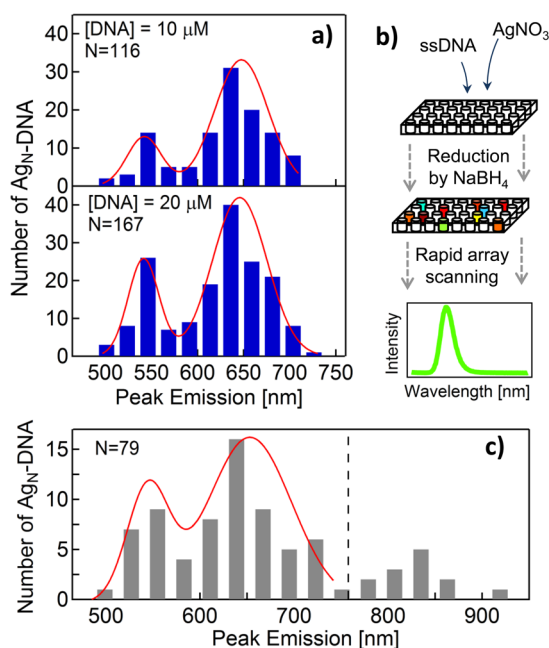


**Figure 1.** (a) Peak fluorescence wavelength histograms for  $\text{Ag}_N\text{-DNA}$  stabilized by randomly generated 10-base oligomers, synthesized at 10  $\mu\text{M}$  DNA and 20  $\mu\text{M}$  DNA with  $\text{Ag}^+:\text{DNA} = 5:1$  and measured 1 week after synthesis to ensure stability of measured products. The number of data,  $N$ , indicated on each graph, represents the number of brightly fluorescent  $\text{Ag}_N\text{-DNA}$  with single-Gaussian spectra that are histogrammed in each plot (see main text). Maximum likelihood estimation fits to a sum of two normal distributions are in red. (b) Cartoon schematic of parallel robotic synthesis and fluorescence characterization. (c) A histogram of published  $\text{Ag}_N\text{-DNA}$  fluorescence wavelengths<sup>6–9,12,13,17,18,21,25–29</sup> is strikingly similar to those resulting from the randomly chosen 10-base strands (Figure 1a).

lineshapes to extract peak fluorescence wavelengths (see Supporting Information). Here we examine results from oligomers that stabilize clusters having (1) fluorescence brightness well above the noise level and (2) single, rather than multiple, fluorescence peaks, corresponding to one

dominant fluorescent product (typically one  $\text{Ag}_N\text{-DNA}$  species formed by a single oligomer under certain synthesis conditions is most desirable for applications<sup>22,23</sup>). Such oligomers comprised up to 25% of the total strand set, depending on synthesis conditions. Apparently sequences producing one dominant fluorescent product are fairly common among randomly selected strands. The remaining 75% of the strands either did not stabilize silver clusters, stabilized “dark” clusters that were not measurably fluorescent, or stabilized clusters that produced very low fluorescent signals due to low chemical yields or quantum yields of fluorescent products. These strands are presumably not favorable hosts for silver clusters, perhaps due to insufficient association to  $\text{Ag}^+$  or because silver clusters stabilized by these strands are not in environments that favor radiative decay.

Histograms of fluorescence wavelengths from single-peak solutions demonstrate bimodal color distributions with enhanced abundances of “green”  $\text{Ag}_N\text{-DNA}$  near 540 nm and “red”  $\text{Ag}_N\text{-DNA}$  near 630 nm (Figure 1a and S2). Although relative heights change somewhat, histogram peaks are invariant over time (one day, one week, and four weeks after synthesis) and synthesis conditions (data for additional synthesis conditions and time points are in Supporting Information), suggesting enhanced stabilities of  $\text{Ag}_N\text{-DNA}$  that possess colors near 540 and 630 nm.<sup>24</sup> The 850 nm sensitivity limit of the well plate reader precludes detection at longer wavelengths.

To investigate whether these color bands are specific to 10-base oligomers, we surveyed results on 79 strands previously reported to form fluorescent  $\text{Ag}_N\text{-DNA}$ ,<sup>6–9,12,13,17,18,21,25–29</sup> with widely varying sequence lengths (6–34 bases) and synthesis conditions. Care was taken to avoid duplicating reported results on identical strands (many oligomers are utilized across multiple studies). A histogram of reported peak fluorescence wavelengths shows a similar color distribution (Figure 1c), with abundances of green and red species as compared to other colors (an additional peak in the near-IR may also indicate a third abundance that is not detectable with our plate reader, which has poor sensitivity beyond  $\sim 750$  nm.) Apparently “magic colors” are generic, rather than special to strands of specific length.

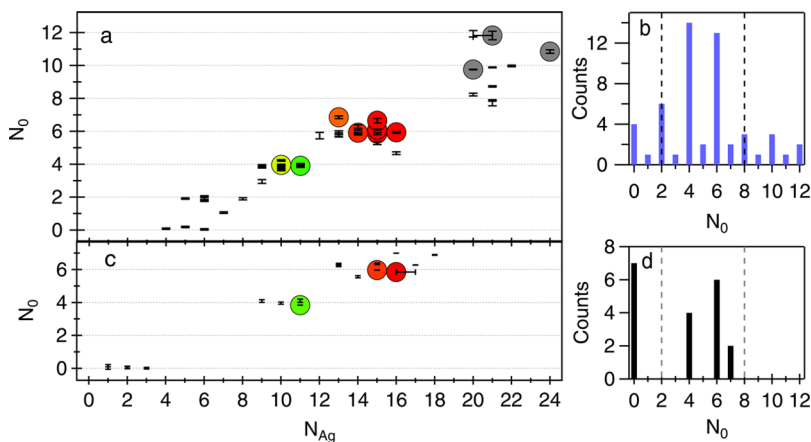


**Figure 2.** (a,b) Neutral Ag atom numbers,  $N_0$ , extracted from previous  $\text{Ag}_N\text{-DNA}$  size data<sup>7</sup> and (c,d) measured for select 10-base well plate strands that produced bright fluorescence and HPLC-stable products. (a,c)  $N_0$  vs  $N$  for HPLC-purified  $\text{Ag}_N\text{-DNA}$ , determined by MS. Brightly fluorescent clusters are indicated by colored dots; RGB colors match fluorescence wavelength (IR-emitting clusters are gray). Black data points represent  $\text{Ag}_N\text{-DNA}$  that were not measurably fluorescent but still sizable by MS. Vertical error bars are standard errors in the cluster charge,  $N_+$ , and horizontal error bars represent uncertainty in  $N$ . (b,d) Histograms of  $N_0$  values show abundances of clusters with even  $N_0$ . Magic numbers predicted by the spherical superatom model (dashed lines) differ from those observed for  $\text{Ag}_N\text{-DNA}$ .

We next consider whether  $\text{Ag}_N\text{-DNA}$  within a “magic color” grouping also share similar cluster properties, regardless of sequence specifics. Previous work used high-performance liquid chromatography with in-line mass spectrometry (HPLC-MS) to identify total numbers of silver atoms,  $N$ , and silver cations,  $N_+$ , for 51 different  $\text{Ag}_N\text{-DNA}$  products<sup>7</sup> that formed on 10 different mixed base sequences with 16–34 bases. From this data we extract the number of neutral silver atoms,  $N_0$ , in each cluster:  $N_0 = N - N_+$  (Figure 2a,b). Distinct groupings are apparent for even  $N_0$ , despite wide-ranging numbers of silver cations (Figure 2a; for  $N_0 = 6$ ,  $N_+$  ranges from 6 to 10). A histogram of  $N_0$  (Figure 2b) displays marked enhancement at even values. Thus, it appears that even magic numbers of  $N_0$  correspond to enhanced abundances of  $\text{Ag}_N\text{-DNA}$  species, regardless of  $N_+$ . Additionally, brightly fluorescent  $\text{Ag}_N\text{-DNA}$  (colored circles in Figure 2a; RGB colors match peak fluorescence) demonstrate color groupings, with green and red clusters grouped separately, mirroring the histogram color peaks in Figure 1b.

We selected three 10-base strands that produced bright fluorescence to investigate whether  $\text{Ag}_N\text{-DNA}$  forming on 10-base template strands also contain the magic numbers of  $N_0$  exhibited in Figure 2a,b and lie in the same magic color bands. Aliquots of the main synthesis products were collected by HPLC separation and examined by negative ion MS (electrospray ionization) (see Supporting Information). Figure 2c,d shows that  $\text{Ag}_N\text{-DNA}$  formed by these strands, both fluorescent and dark, indeed shows an overwhelming propensity for even  $N_0$ , and that colors lie in the same bands exhibited in Figure 2a. (If the neutral silver atoms were not included in a single cluster, there would be no reason for color to red-shift with larger  $N_0$ , a trend that is clear in Figure 2 and is discussed in more detail in ref 7).

To better understand the magic nature of certain  $N_0$  rather than certain  $N$ , we consider the well-studied spherical, ligand-stabilized gold clusters.<sup>5</sup> In these “superatoms,” total Au atom number,  $N$ , is not magic because ligands effectively remove some gold atoms from the cluster.<sup>5</sup> For thiolate- and phosphine-stabilized Au clusters, ligands bind to surface Au atoms and withdraw a fraction of the cluster’s electrons, forming protective units around the cluster and leaving behind a magic number of electrons, and thus *neutral* gold atoms, in the cluster core.<sup>4,5</sup> Magic numbers of these core electrons are predicted by electronic shell closings in the spherical “superatom” model. While ligand-stabilized silver clusters developed much later than their gold counterparts,<sup>30,31</sup> the existence of magic number silver clusters was recently established using thiolate ligands.<sup>32–34</sup>

For DNA-stabilized silver clusters, the most prominent magic numbers of neutral Ag atoms observed are 4 and 6 (Figure 2), not 2 and 8 as predicted by the spherical “superatom” model (dashed lines, Figure 2b,d). For nonspherical clusters, superatom magic numbers no longer hold special significance due to lifting of degeneracies by spherical symmetry breaking,<sup>35</sup> such as cluster reshaping by ligand–metal interactions.<sup>36</sup> Instead, the ellipsoidal shell model predicts even–odd oscillation of stability as a function of metal cluster atom number,<sup>35</sup> as we observe in Figure 2. The distinct magic numbers of  $\text{Ag}_N\text{-DNA}$ , relative to spherical gold clusters, thus indicate nonspherical cluster shapes.

Because silver cations are thought to bind to ring nitrogens in DNA bases,<sup>6,27</sup> we infer that base- $\text{Ag}^+$  complexes act as ligand units, analogous to thiolate- and phosphine-bonded Au units.

One crucial difference is that DNA presents multiple base ligands arrayed along a line-like backbone, which could favor elongated, rod-like cluster shapes, as are also needed to account for the optical properties of  $\text{Ag}_N\text{-DNA}$ .<sup>7</sup> This suggests a quasi-linear perimeter of base-attached  $\text{Ag}^+$  around a rod-like cluster that exhibits enhanced abundances at even magic numbers of neutral Ag atoms.

We now turn to the relation between color distribution and magic numbers.  $\text{Ag}_N\text{-DNA}$  from the two prominent peaks in Figure 1a, centered at 540 and 630 nm, respectively, fall within the high abundances of clusters having  $N_0 = 4$  and  $N_0 = 6$ , respectively (Figure 2c). We thus infer that “magic” green clusters within the 540 nm color band correspond to  $\text{Ag}_N\text{-DNA}$  with  $N_0 = 4$ , and “magic” red clusters within the 630 nm color band correspond to  $\text{Ag}_N\text{-DNA}$  with  $N_0 = 6$ . This is consistent with a previously established trend of longer wavelength fluorescence for  $\text{Ag}_N\text{-DNA}$  with larger silver clusters<sup>9</sup> and also agrees with the previously sized fluorescent clusters in Figure 2a: the 7 fluorescent clusters with  $N_0 = 6$  emit within 60 nm of the 630 nm color peak, and the 3 fluorescent clusters with  $N_0 = 4$  emit within 25 nm of the 540 nm color peak. Additional IR emitters in Figure 2a, corresponding to the near-IR band in Figure 1c, may indicate another magic  $N_0$ . IR emitters stabilized by the 10-base random strands were not detectable with the plate reader, however, so we make no conjectures here as to the value of  $N_0$  for this abundance.

The 540 and 630 nm histogram peaks (Figure 1a) have standard deviations of 20 and 30 nm, respectively. To understand why the peaks corresponding to magic  $N_0$  are so wide, we consider the well-known sensitivity of transition wavelengths of rod-shaped clusters to cluster aspect ratio and bending. Thus, a range of aspect ratios and/or curvatures could qualitatively account for observed color spreads at magic  $N_0$ . We expect base- $\text{Ag}^+$  units to influence color by determining cluster shape. The existence of dark  $\text{Ag}_N\text{-DNA}$  with  $N_0 = 0$  and up to six  $\text{Ag}^+$  (Figure 2a) shows that fluorescent clusters may also contain  $\text{Ag}^+$  that are not incorporated into the base- $\text{Ag}^+$  ligand units surrounding the neutral cluster core.  $\text{Ag}^+$  content varies from  $N_+ = 6$ –9 in red-emitting clusters with  $N_0 = 6$ , suggesting that up to three  $\text{Ag}^+$  are associated with bases detached from the cluster, where they may still affect wavelength by altering the potential seen by the cluster’s delocalized electrons.

Figure 3 shows variants on such a silver cluster nanorod, adapted from previously suggested structures,<sup>7,37</sup> (AMBER structure generation details in the Supporting Information<sup>38–43</sup>). Like ligand-protected Au clusters, base- $\text{Ag}^+$  units protect a neutral cluster core containing a magic number of neutral silver atoms, even  $N_0$ , due to spin degeneracy (Figure 3a,b). Ag–Ag bond angle variation within the core can produce a range of aspect ratios for a fixed  $N_0$ , avoiding energetically costly changes in Ag bond length caused by modifying Ag bond angles and base stacking energies. Molecular dynamics simulations<sup>38</sup> show that clusters may assume curved shapes due to Coulomb interactions, and addition or subtraction of silver ions near the cluster can modify cluster shape (Figure 3c,d). We expect that a combination of such shape factors account for the breadth of histogram peaks in Figure 1b.

Finally, we consider the specificity of  $\text{Ag}_N\text{-DNA}$  color to the particular DNA template sequence, an important issue for  $\text{Ag}_N\text{-DNA}$  colorimetric sensing schemes. Our array data studies show that many distinct sequences produce nearly the same fluorescence color. In particular, for red emitters we find 26



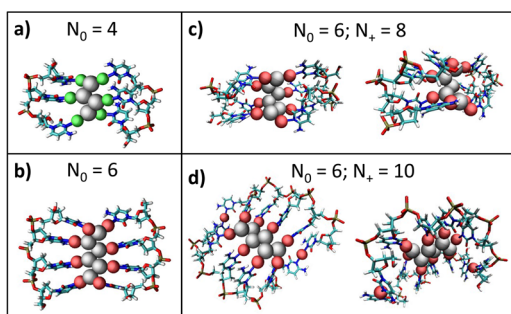


**Figure 3.** Cluster schematics from AMBER simulations for (a) a green-emitting  $N_0 = 4$   $\text{Ag}_N$ -DNA and (b) a red-emitting  $N_0 = 6$   $\text{Ag}_N$ -DNA. (c) AMBER simulations of the  $N_0 = 6$  cluster structure after 1 ns for with front and side views, as compared to (b). Simulations suggest that  $\text{Ag}_N$ -DNA may assume curved shapes, influenced by location of Ag ions. (d) Simulations of a  $N_0 = 6$ ,  $N_+ = 10$  cluster structure after 1 ns. Additional Ag ions that are not directly bound to the cluster's neutral core but still associated with the  $\text{Ag}_N$ -DNA complex may cause additional shape and/or fluorescence wavelength changes, as seen by comparing the shapes of  $N_0 = 6$  clusters with 8  $\text{Ag}^+$  (Figure 3c) to  $N_0 = 6$  clusters with 10  $\text{Ag}^+$  (Figure 3c).

distinct ten-base strands that produce the same peak fluorescence color to within 10 nm (see Supporting Information). This will challenge the development of sensing schemes aimed at distinguishing the presence of specific sequences amidst a background of other DNA.

In conclusion, we observe significantly enhanced abundances of  $\text{Ag}_N$ -DNA stabilized by random DNA oligomers with fluorescence peaks near 540 and 630 nm. HPLC-MS data shows that these color groupings correspond to cluster populations with even numbers of neutral silver atoms, different from magic numbers for spherical clusters. Due to the dependence of fluorescence wavelength on neutral silver atom number, magic numbers of silver atoms result in “magic color” bands. Variants on rod-like cluster models qualitatively explain the breadth of the color histogram peaks relative to magic numbers by permitting variations in cluster length and immediate environment. The existence of such “magic colors” has implications for the palette available to colorimetric assays and could be exploited in sensing applications where transitions between green and red emissive clusters act as signals for a desired process.

## EXPERIMENTAL METHODS

**Parallel Cluster Synthesis.** Random 10-base DNA sequences were generated by a MATLAB random number generator, excluding sequences with fewer than 3 C plus G bases. Well-plate format DNA was ordered presuspended in water with standard desalting from Integrated DNA Technologies. Several wells contained a control oligomer known to produce bright fluorescence to confirm proper synthesis. A Beckman Coulter Biomek 2000 pipetting robot was used to synthesize  $\text{Ag}_N$ -DNA at four synthesis conditions: 10  $\mu\text{M}$  and 20  $\mu\text{M}$  DNA, with  $[\text{AgNO}_3]/[\text{DNA}] = 5$  and 10. Synthesis was performed at pH 7 in 10 mM  $\text{NH}_4\text{OAc}$ , with  $[\text{NaBH}_4]/[\text{AgNO}_3] = 0.5$ . See Supporting Information for details.

**Spectral Characterization and Histogram Fitting.** Fluorescence spectra were measured using a Tecan Infinite 200 PRO reader and fitted to single Gaussians as a function of energy to extract spectral parameters using Igor Pro 6, Wavemetrics.  $\text{Ag}_N$ -DNA solutions with dim fluorescence or multiple peaks were

excluded from histograms (see Supporting Information for details). Maximum likelihood estimation fits to bimodal distributions were performed using MATLAB R2012a.

**Mass Spectrometry of Silver Clusters.** Synthesis of select bright  $\text{Ag}_N$ -DNA was scaled to 1 mL, and products were purified by HPLC and sized by MS to obtain total silver content,  $N$ , and the number of silver cations,  $N_+$ . For details and spectra, see Supporting Information.

## ASSOCIATED CONTENT

### Supporting Information

DNA template sequence generation, robotic synthesis procedure, spectral fitting details, additional cluster color histograms and fitting details, MS spectra for HPLC-purified  $\text{Ag}_N$ -DNA, and AMBER simulation details for cluster structures. This material is available free of charge via the Internet at <http://pubs.acs.org>.

## AUTHOR INFORMATION

### Corresponding Author

\*E-mail: [bgwinn@physics.ucsb.edu](mailto:bgwinn@physics.ucsb.edu).

### Notes

The authors declare no competing financial interest.

## ACKNOWLEDGMENTS

This work was funded by NSF grants CHE-1213895 and DMR-1309410. S.M.C. acknowledges support from NSF-DGE-1144085 (NSF Fellowship). We acknowledge use of the Biological Nanostructures Laboratory in the CNSI and MRL: an NSF MRSEC (DMR-1121053). S.M.C. and E.G. thank Lincoln Johnson for use of the pipetting robot acquired with support from NIH-NEI 5-R24-EY14799, and Monte Radeke for his invaluable assistance in programming the robot.

## REFERENCES

- (1) Schön, G.; Simon, U. A Fascinating New Field in Colloid Science: Small Ligand-Stabilized Metal Clusters and Possible Application in Microelectronics. *Colloid Polym. Sci.* **1995**, *273*, 101–117.
- (2) Daniel, M.-C.; Astruc, D. Gold Nanoparticles: Assembly, Supramolecular Chemistry, Quantum-Size-Related Properties, and Applications toward Biology, Catalysis, and Nanotechnology. *Chem. Rev.* **2004**, *104*, 293–346.
- (3) Toshima, N.; Shiraishi, Y.; Teranishi, T.; Miyake, M.; Tominaga, T.; Watanabe, H.; Brijoux, W.; Bönnemann, H.; Schmid, G. Various Ligand-Stabilized Metal Nanoclusters as Homogeneous and Heterogeneous Catalysts in the Liquid Phase. *Appl. Organomet. Chem.* **2001**, *15*, 178–196.
- (4) Jadzinsky, P. D.; Calero, G.; Ackerson, C. J.; Bushnell, D. A.; Kornberg, R. D. Structure of a Thiol Monolayer-Protected Gold Nanoparticle at 1.1 Å Resolution. *Science* **2007**, *318*, 430–433.
- (5) Walter, M.; Akola, J.; Lopez-Acevedo, O.; Jadzinsky, P. D.; Calero, G.; Ackerson, C. J.; Whetten, R. L.; Grönbeck, H.; Häkkinen, H. A Unified View of Ligand-Protected Gold Clusters as Superautom Complexes. *Proc. Natl. Acad. Sci. U. S. A.* **2008**, *105*, 9157–9162.
- (6) Petty, J. T.; Zheng, J.; Hud, N. V.; Dickson, R. M. DNA-Templated Ag Nanocluster Formation. *J. Am. Chem. Soc.* **2004**, *126*, 5207–5212.
- (7) Schultz, D.; Gardner, K.; Oemrawsingh, S. S. R.; Markešević, N.; Olsson, K.; Debord, M.; Bouwmeester, D.; Gwinn, E. Evidence for Rod-Shaped DNA-Stabilized Silver Nanocluster Emitters. *Adv. Mater.* **2013**, *25*, 2797–2803.
- (8) Petty, J. T.; Fan, C.; Story, S. P.; Sengupta, B.; Iyer, A. S. J.; Prudowsky, Z.; Dickson, R. M. DNA Encapsulation of Ten Silver

Atoms Produces a Bright, Modulatable, Near Infrared-Emitting Cluster. *J. Phys. Chem. Lett.* **2010**, *1*, 2524–2529.

(9) Schultz, D.; Gwinn, E. G. Silver Atom and Strand Numbers in Fluorescent and Dark Ag:DNAs. *Chem. Commun. (Camb.)* **2012**, *48*, 5748–5750.

(10) O'Neill, P. R.; Gwinn, E. G.; Fyngenson, D. K. UV Excitation of DNA Stabilized Ag Cluster Fluorescence via the DNA Bases. *J. Phys. Chem. C* **2011**, *115*, 24061–24066.

(11) Vosch, T.; Antoku, Y.; Hsiang, J.-C.; Richards, C. I.; Gonzalez, J. I.; Dickson, R. M. Strongly Emissive Individual DNA-Encapsulated Ag Nanoclusters as Single-Molecule Fluorophores. *Proc. Natl. Acad. Sci. U. S. A.* **2007**, *104*, 12616–12621.

(12) Guo, W.; Yuan, J.; Wang, E. Oligonucleotide-Stabilized Ag Nanoclusters as Novel Fluorescence Probes for the Highly Selective and Sensitive Detection of the Hg<sup>2+</sup> Ion. *Chem. Commun. (Cambridge, U. K.)* **2009**, 3395–3397.

(13) Lan, G.-Y.; Huang, C.-C.; Chang, H.-T. Silver Nanoclusters as Fluorescent Probes for Selective and Sensitive Detection of Copper Ions. *Chem. Commun. (Cambridge, U. K.)* **2010**, *46*, 1257–1259.

(14) Shah, P.; Rørvig-Lund, A.; Chaabane, S. Ben; Thulstrup, P. W.; Kjaergaard, H. G.; Fron, E.; Hofkens, J.; Yang, S. W.; Vosch, T. Design Aspects of Bright Red Emissive Silver nanoclusters/DNA Probes for microRNA Detection. *ACS Nano* **2012**, *6*, 8803–8814.

(15) Liu, Y.; Zhang, M.; Yin, B.; Ye, B. Attomolar Ultrasensitive MicroRNA Detection by DNA-Scaffolded Silver-Nanocluster Probe Based on Isothermal Amplification. *Anal. Chem.* **2012**, *84*, 5165–5169.

(16) Petty, J. T.; Sengupta, B.; Story, S. P.; Degtyareva, N. N. DNA Sensing by Amplifying the Number of Near-Infrared Emitting, Oligonucleotide-Encapsulated Silver Clusters. *Anal. Chem.* **2011**, *83*, 5957–5964.

(17) Guo, W.; Yuan, J.; Dong, Q.; Wang, E. Highly Sequence-Dependent Formation of Fluorescent Silver Nanoclusters in Hybridized DNA Duplexes for Single Nucleotide Mutation Identification. *J. Am. Chem. Soc.* **2010**, *132*, 932–934.

(18) Yeh, H.-C.; Sharma, J.; Shih, I.-M.; Vu, D. M.; Martinez, J. S.; Werner, J. H. A Fluorescence Light-Up Ag Nanocluster Probe That Discriminates Single-Nucleotide Variants by Emission Color. *J. Am. Chem. Soc.* **2012**, *134*, 11550–11558.

(19) Sengupta, B.; Ritchie, C. M.; Buckman, J. G.; Johnsen, K. R.; Goodwin, P. M.; Petty, J. T. Base-Directed Formation of Fluorescent Silver Clusters. *J. Phys. Chem. C* **2008**, 18776–18782.

(20) Yeh, H.-C.; Sharma, J.; Han, J. J.; Martinez, J. S.; Werner, J. H. A DNA–Silver Nanocluster Probe That Fluoresces upon Hybridization. *Nano Lett.* **2010**, *10*, 3106–3110.

(21) Schultz, D.; Gwinn, E. Stabilization of Fluorescent Silver Clusters by RNA Homopolymers and Their DNA Analogs: C,G versus A,T(U) Dichotomy. *Chem. Commun. (Cambridge, U. K.)* **2011**, *47*, 4715–4717.

(22) Richards, C. I.; Choi, S.; Hsiang, J.-C.; Antoku, Y.; Vosch, T.; Bongiorno, A.; Tzeng, Y.-L.; Dickson, R. M. Oligonucleotide-Stabilized Ag Nanocluster Fluorophores. *J. Am. Chem. Soc.* **2008**, *130*, 5038–5039.

(23) Sharma, J.; Yeh, H.-C.; Yoo, H.; Werner, J. H.; Martinez, J. S. A Complementary Palette of Fluorescent Silver Nanoclusters. *Chem. Commun. (Cambridge, U. K.)* **2010**, *46*, 3280–3282.

(24) Desiredy, A.; Kumar, S.; Guo, J.; Bolan, M. D.; Griffith, W. P.; Bigioni, T. P. Temporal Stability of Magic-Number Metal Clusters: Beyond the Shell Closing Model. *Nanoscale* **2013**, *5*, 2036–2044.

(25) Gwinn, E. G.; O'Neill, P.; Guerrero, A. J.; Bouwmeester, D.; Fyngenson, D. K. Sequence-Dependent Fluorescence of DNA-Hosted Silver Nanoclusters. *Adv. Mater.* **2008**, *20*, 279–283.

(26) Neill, P. R. O.; Velazquez, L. R.; Dunn, D. G.; Gwinn, E. G.; Fyngenson, D. K. Hairpins with Poly-C Loops Stabilize Four Types of Fluorescent Ag:DNA. *J. Phys. Chem. C* **2009**, *113*, 4229–4233.

(27) Ritchie, C. M.; Johnsen, K. R.; Kiser, J. R.; Antoku, Y.; Dickson, R. M.; Petty, J. T. Ag Nanocluster Formation Using a Cytosine Oligonucleotide Template. *J. Phys. Chem. C* **2007**, *111*, 175–181.

(28) Petty, J. T.; Fan, C.; Story, S. P.; Sengupta, B.; Sartin, M.; Hsiang, J.-C.; Perry, J. W.; Dickson, R. M. Optically Enhanced, Near-

IR, Silver Cluster Emission Altered by Single Base Changes in the DNA Template. *J. Phys. Chem. B* **2011**, *115*, 7996–8003.

(29) Han, B.; Wang, E. Oligonucleotide-Stabilized Fluorescent Silver Nanoclusters for Sensitive Detection of Biothiols in Biological Fluids. *Biosens. Bioelectron.* **2011**, *26*, 2585–2589.

(30) Farrag, M.; Thämer, M.; Tschurl, M.; Bürgi, T.; Heiz, U. Preparation and Spectroscopic Properties of Monolayer-Protected Silver Nanoclusters. *J. Phys. Chem. C* **2012**, *116*, 8034–8043.

(31) Udayabhaskararao, T.; Pradeep, T. New Protocols for the Synthesis of Stable Ag and Au Nanocluster Molecules. *J. Phys. Chem. Lett.* **2013**, *4*, 1553–1564.

(32) Desiredy, A.; Conn, B. E.; Guo, J.; Yoon, B.; Barnett, R. N.; Monahan, B. M.; Kirschbaum, K.; Griffith, W. P.; Whetten, R. L.; Landman, U.; et al. Ultraprecise Silver Nanoparticles. *Nature* **2013**, *501*, 399–402.

(33) Yang, H.; Wang, Y.; Huang, H.; Gell, L.; Lehtovaara, L.; Malola, S.; Häkkinen, H.; Zheng, N. All-Thiol-Stabilized Ag<sub>44</sub> and Au<sub>12</sub>Ag<sub>32</sub> Nanoparticles with Single-Crystal Structures. *Nat. Commun.* **2013**, *4*, 2422.

(34) Yang, H.; Lei, J.; Wu, B.; Wang, Y.; Zhou, M.; Xia, A.; Zheng, L.; Zheng, N. Crystal Structure of a Luminescent Thiolated Ag Nanocluster with an Octahedral Ag<sub>6</sub><sup>4+</sup> Core. *Chem. Commun. (Cambridge, U. K.)* **2013**, *49*, 300–302.

(35) De Heer, W. The Physics of Simple Metal Clusters: Experimental Aspects and Simple Models. *Rev. Mod. Phys.* **1993**, *65*, 611–676.

(36) Dhillon, H.; Fournier, R. Geometric Structure of Silver Clusters with and without Adsorbed Cl and Hg. *Comput. Theor. Chem.* **2013**, *1021*, 26–34.

(37) Ramazanov, R. R.; Kononov, A. I. Excitation Spectra Argue for Threadlike Shape of DNA-Stabilized Silver Fluorescent Clusters. *J. Phys. Chem. C* **2013**, *117*, 18681–18687.

(38) Case, D. A.; Darden, T. A.; Cheatham, III, T. E.; Simmerling, C. L.; Wang, J.; Duke, R. E.; Luo, R.; Walker, R. C.; Zhang, W.; Merz, K. M.; et al. AMBER 12, 2012.

(39) Walker, R. Simulating a Solvated Protein that Contains Non-Standard Residues (Simple Version) [http://ambermd.org/tutorials/advanced/tutorial11\\_orig/](http://ambermd.org/tutorials/advanced/tutorial11_orig/).

(40) Humphrey, W.; Dalke, A.; Schulten, K. VMD: Visual Molecular Dynamics. *J. Mol. Graph.* **1996**, *14*, 33–38.

(41) Soto-Verdugo, V.; Metiu, H.; Gwinn, E. The Properties of Small Ag Clusters Bound to DNA Bases. *J. Chem. Phys.* **2010**, *132*, 195102.

(42) Wu, D. Y.; Hayashi, M.; Shiu, Y. J.; Liang, K. K.; Chang, C. H.; Yeh, Y. L.; Lin, S. H. A Quantum Chemical Study of Bonding Interaction, Vibrational Frequencies, Force Constants, and Vibrational Coupling of Pyridine–M<sub>n</sub> (M = Cu, Ag, Au; n = 2–4). *J. Phys. Chem. A* **2003**, *107*, 9658–9667.

(43) Lin, F.; Wang, R. Systematic Derivation of AMBER Force Field Parameters Applicable to Zinc-Containing Systems. *J. Chem. Theory Comput.* **2010**, *6*, 1852–1870.